ISSN 1674-1056
http://cpb.iphy.ac.cn
http://iopscience.iop.org/cpb
中国物理 B
Chinese Physics
中国物理
Chinese Physics B

Laser-assisted Stark deceleration of CaF in its rovibronic ground (high-field-seeking) state

Yuefeng Gu(顾跃凤), Kai Chen(陈凯), Yunxia Huang(黄云霞), Xiaohua Yang(杨晓华)

Citation: Chin. Phys. B . 2019, 28(4): 043702. **doi:** 10.1088/1674-1056/28/4/043702
Journal homepage: http://cpb.iphy.ac.cn; http://iopscience.iop.org/cpb

What follows is a list of articles you may be interested in

Optical Stark deceleration of neutral molecules from supersonic expansion with a rotating laser beam

Yongcheng Yang(杨永成), Shunyong Hou(侯顺永), Lianzhong Deng(邓联忠)
Chin. Phys. B . 2018, 27(5): 053701. **doi:** 10.1088/1674-1056/27/5/053701

Combination of multiple tools for surface manipulation of polar molecules

Qiang Wang(王强), Bin Wei(魏斌), Heng-Jiao Guo(郭恒娇), Sheng-Qiang Li(李胜强), Shun-Yong Hou(侯顺永), Jian-Ping Yin(印建平)
Chin. Phys. B . 2017, 26(11): 113701. **doi:** 10.1088/1674-1056/26/11/113701

Theoretical derivation and simulation of a versatileelectrostatic trap for cold polar molecules

Shengqiang Li(李胜强)
Chin. Phys. B . 2016, 25(11): 113702. **doi:** 10.1088/1674-1056/25/11/113702

Adiabatic cooling for cold polar molecules on a chip using a controllable high-efficiency electrostatic surface trap

Li Sheng-Qiang, Xu Liang, Xia Yong, Wang Hai-Ling, Yin Jian-Ping
Chin. Phys. B . 2014, 23(12): 123701. **doi:** 10.1088/1674-1056/23/12/123701

Electrostatic surface trap for cold polar molecules on a chip

Wang Qin, Li Sheng-Qiang, Hou Shun-Yong, Xia Yong, Wang Hai-Ling, Yin Jian-Ping
Chin. Phys. B . 2014, 23(1): 013701. **doi:** 10.1088/1674-1056/23/1/013701

Laser-assisted Stark deceleration of CaF in its rovibronic ground (high-field-seeking) state*

Yuefeng Gu(顾跃凤)[1], Kai Chen(陈凯)[1], Yunxia Huang(黄云霞)[1,†], and Xiaohua Yang(杨晓华)[1,2,‡]

[1] *School of Science, Nantong University, Nantong* 226019, *China*

[2] *State Key Laboratory of Precision Spectroscopy, East China Normal University, Shanghai* 200062, *China*

(Received 10 December 2018; revised manuscript received 29 January 2019; published online 5 March 2019)

A near-resonant, red-detuning laser-assisted Stark deceleration scheme is proposed to slow CaF in its high-field-seeking rovibronic ground state. The assisting Gaussian laser beam can confine CaF molecules transversely owing to the optical Stark effect. Simulations suggest that the present scheme is superior to previous Stark decelerators. Under typical experimental conditions, when the assisting laser frequency is red-detuned to the molecular transition ($\lambda \sim 606.3$ nm) by 5.0 GHz and the laser power is about 5.6 W, the proposed decelerator can achieve a total number at the order of 10^4 CaF molecules with a number density at the order of 10^8 cm^{-3}. The equivalent temperature of the obtained cold CaF molecules is 2.3 mK. Additionally, the desired assisting laser power can be as low as about 1.2 W if keeping the red-detuning value to be 1.0 GHz, which further suggests its experimental feasibility.

Keywords: Stark deceleration, polar molecule, optical Stark effect, high-field-seeking state

PACS: 37.10.Mn, 32.60.+i **DOI:** 10.1088/1674-1056/28/4/043702

1. Introduction

For about two decades, cold molecules ($T < 1$ K) have gained increasing attention of researchers in a variety of fields due to their wide applications in quantum simulation,[1,2] quantum information,[3–5] quantum chemistry,[6,7] and precision measurements.[8–11] Complex internal structure of molecules, related to their vibrational and rotational internal motions, and also fine and hyperfine interactions, makes molecules good candidates for quantum engineering of chemistry and quantum matter investigations[12] despite the difficulty of producing cold molecules. Additionally, polar molecules are of particular importance due to their long-range and anisotropic interactions.[13,14]

Various methods have been developed to cool molecules, such as direct laser cooling,[15–17] Stark deceleration,[18–21] Zeeman deceleration,[22–24] buffer gas cooling combined with bending guiding,[25,26] opto-electrical cooling,[27,28] and magneto-optical trapping and cooling.[29–32] Specifically, Stark deceleration is versatile for chemically stable polar molecules and can achieve large total number and high number density of cold molecules. Unfortunately, traditional Stark deceleration works only for low-field-seeking (LFS) molecules[33,34] while most chemically stable molecules are high-field-seeking (HFS) in their rovibronic ground state. Bethlem *et al.*[35] developed the alternating gradient (AG) Stark decelerator for HFS molecules, which was employed by Wall *et al.*[36] to decelerate calcium monofluoride (CaF). However, the AG decelerator is hard to align, and either the relative molecular number or the deceleration efficiency is much lower than traditional Stark decelerator. Recently, Huang *et al.*[37] proposed a far-red-detuning laser-assisted Stark deceleration scheme to decelerate the HFS iodine chloride (ICl) molecule. Simulation suggested that lower velocity and higher number density of cold molecules could be obtained using the new deceleration scheme. However, it requires a high-power assisting laser, which makes the experiment more challenging. Later, Chen *et al.*[38] suggested to decelerate the linear $HC_{2n+1}N$ ($n = 2$, 3, and 4) molecules using the new scheme. For these molecules, the required laser intensity is only 10% of that for ICl. Nevertheless, the required laser intensity is too high and not practical.

In the present work, we propose to use a near-resonant, red-detuning laser beam in place of the far-detuning one as the assisting laser to slow CaF in its rovibronic ground (HFS) state. As the near-red-detuning laser beam can provide enough transverse guiding potential to the HFS CaF molecules at low laser power (< 10 W), the present deceleration scheme is more feasible. Our simulation suggests that CaF can be slowed to rest in the laboratory frame within 100 Stark-deceleration stages with both high number and high density. Consequently, the decelerated CaF molecules would have wider applications in the field of cold molecules. They can also be further cooled to obtain ultracold molecules.

*Project supported by the National Natural Science Foundation of China (Grant No. 11604164).

†Corresponding author. E-mail: hyx@ntu.edu.cn

‡Corresponding author. E-mail: xhyang@ntu.edu.cn

© 2019 Chinese Physical Society and IOP Publishing Ltd

2. Decelerator and theory

The proposed near-resonant, red-detuning laser-assisted Stark deceleration apparatus for decelerating CaF molecules in HFS states is shown in Fig. 1. It is similar to the far-red-detuning decelerator that was described in detail previously.[37,38] The left part is a traditional Stark decelerator merely omitting the electrostatic hexapole LFS molecular focalizer. The production of CaF free radicals may follow the method of Zhelyazkova *et al.*[16] Briefly, sulfur hexafluoride (SF_6) seeded in xenon at a backing pressure of about one atmosphere is supersonically expanded into a vacuum chamber through a pulsed valve. Free Ca atoms, ablated by a pulsed second harmonic Nd:YAG laser from a calcium disk located downstream the valve, react with SF_6 to form CaF molecules. The produced CaF molecules pass through a skimmer with a diameter of 0.1 mm (matching the assisting laser beam) to form a molecular beam. Subsequently, the CaF molecular beam passes through a set of deceleration stages. The stages are equally spaced at 5.0-mm with the first stage locating 5.0 mm downstream the skimmer. Each stage consists of two stainless steel rods spaced by 2.0 mm, and ±10-kV high voltages are applied on the electrode pair to produce 100-kV/cm electrostatic field at the center.

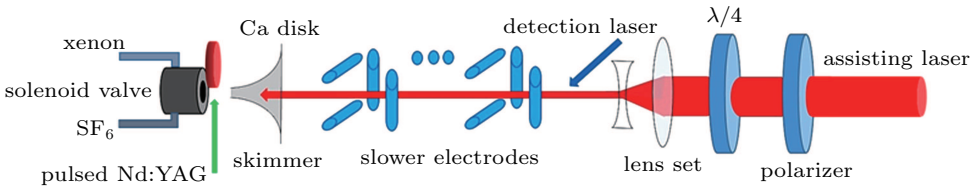


Fig. 1. Proposed experimental apparatus scheme for the near-resonant, red-detuning laser-assisted Stark deceleration of CaF in its high-field-seeking state. See text for details.

A circularly polarized, near-red-detuning assisting Gaussian laser beam ($\lambda \sim 606.3$ nm), is collimated into 0.1 mm in diameter at its beam waist. The focused laser beam waist follows the molecular package of interest by adjusting the lens set synchronously. The collimated laser beam counter-propagates against the CaF molecular beam to transversely confine the CaF beam owing to optical Stark effect. Note that circular polarization is required to avoid the orientation effect,[37] which would complicate the slowing process. And finally, the decelerated CaF molecules can be detected downstream the stages via either laser-induced fluorescence spectroscopy or resonance-enhanced multi-photon ionization spectroscopy.

In the rigid rotator model, the Hamiltonian of CaF in the laser-assisted Stark decelerator is as follows,

$$H = BN(N+1) + \gamma N \cdot S - \mu E \cos\theta + V, \tag{1}$$

where B is the molecular rotational constant, N is the rotational angular momentum quantum number, γ is the spin-rotational coupling constant, μ is the molecular electric dipole, θ is the angle between μ and the electrostatic field (E), and V is the optical Stark potential for interaction between the CaF molecule and the laser field.

The Stark shift of the level j of the molecule in a near-resonant laser field $E_{\rm L}$ is given by[39]

$$V_j = -\frac{1}{4h}\sum_i |\langle i|\boldsymbol{E}_{\rm L}\cdot\boldsymbol{\mu}|j\rangle|^2\left(\frac{1}{\nu_{ij}-\nu}+\frac{1}{\nu_{ij}+\nu}\right), \tag{2}$$

where i denotes the upper level allowed to decay to the lower level j, h is Planck constant, ν is the frequency of the laser beam, ν_{ij} is the transition frequency. In the near-resonant case, V_j can be approximated as follows:

$$V_j = -\frac{1}{4h}\sum_i \frac{|\langle i|E_{\rm L}\cdot\mu|j\rangle|^2}{\nu_{ij}-\nu}. \tag{3}$$

Therefore, the optical Stark potential of the rovibronic ground state CaF in the assisting laser beam is

$$V = -\frac{q_{00}d^2E_{\rm L}^2}{4h}\sum_i \frac{f_i\cdot S_J}{\nu_{ij}-\nu}, \tag{4}$$

where ν_{ij} is the rotational spectral frequency of the (0, 0) band in the $A^2\Pi_{1/2}$–$X^2\Sigma^+$ (A–X) system of CaF, d is the transition dipole moment, q_{00} is the Franck–Condon factor of the (0, 0) band, f_i is the degeneracy of the state i, and S_J is the Hönl–London factor of the transition. Note that, the contributions of the transitions in the other bands are little due to both their small Franck–Condon factors and large detuning frequencies ($\nu_{ij}-\nu$), and thus neglected.

3. Results and discussion

The CaF molecular parameters of interest in the present work are as follows: the rotational constant $B = 0.3385$ cm^{-1},[40] the spin-rotational coupling constant $\gamma = 0.00131$ cm^{-1},[41] the molecular dipole moment $\mu = 3.07$ D,[42] and the Franck–Condon factor $q_{00} = 0.987$,[43] and the transition dipole moment $d = 5.95$ D[44] for the A–X system.

The energy level diagram of CaF molecule is illustrated in Fig. 2, where $+/-$ denotes the parity of the Lambda-doublets

in the upper state. The rovibronic ground state is of + parity. Limited by the parity-related selection rule ($+ \leftrightarrow -$), of all the transitions originating from the rovibronic ground state, only the $|J' = 3/2, -\rangle \leftarrow |J'' = 1/2\rangle$ (*i.e.*, $R(1/2)$) and $|J\prime = 1/2, -\rangle \leftarrow |J'' = 1/2\rangle$ (*i.e.*, $Q(1/2)$) transitions (green), are allowed, while the others (to the + parity levels) are forbidden. Note that the hyperfine structure is not resolved in the diagram (Fig. 2) because they are on the order of tens of MHz,[16,45] which is much less than the Lambda-splitting.

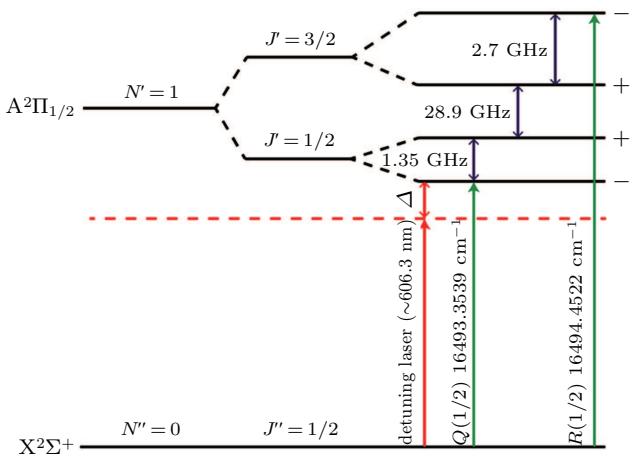


Fig. 2. Energy-level diagram of the CaF molecule (not to scale) and related transitions. Green arrows denote allowed transitions. The red arrow represents the assisting laser red-detuned to the $|J' = 1/2, -\rangle \leftarrow |J'' = 1/2\rangle$ ($Q(1/2)$) transition by Δ.

Calculated Stark potentials of the $|N, M\rangle = |0, 0\rangle$ and $|4, 0\rangle$ sub-levels in the vibronic ground state of CaF as a function of the applied electric field is illustrated in Fig. 3. It shows that the $|0, 0\rangle$ sub-level is HFS while the $|4, 0\rangle$ sub-level is LFS. Stark shift of the former level is ~ 6.2 times stronger of that of the latter (see inset of Fig. 3). Therefore, $|0, 0\rangle$ is used to simulate the proposed laser-assisted Stark deceleration scheme and $|4, 0\rangle$ is used to simulate the traditional scheme[18] for comparison. Note that, the $|4, 0\rangle$ sub-level has the maximum Stark shift among all LFS states.[36]

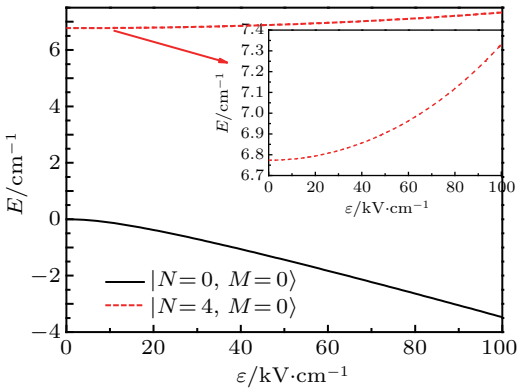


Fig. 3. Stark shift of $|N = 0, M = 0\rangle$ and $|N = 4, M = 0\rangle$ levels in the vibronic ground state of CaF as a function of the applied electrostatic field.

When the molecules pass through the decelerator, they experience an inhomogeneous electric field, resulting in varying Stark shifts of the levels. As indicated in Eq. (4), the optical Stark effect in the assisting laser field depends strongly on the frequency detuning. However, will the optical Stark effect be affected by the inhomogeneous electric field experienced by the molecules when they travel in the decelerator? The answer is nearly negative. Figure 4(a) plots the Stark sublevels of interest varying with the electric field and the arrows denote the transitions that contribute to the optical Stark effect. As shown in Fig. 2, when the assisting laser frequency (red arrow) is red-detuned to $Q(1/2)$ by $\Delta = 5.0$ GHz, it is red-detuned to $R(1/2)$ by ~ 38 GHz. Thus, the $R(1/2)$ transition has less contribution to the optical Stark effect. Furthermore, the frequency of the $Q(1/2)$ transition is invariable in the electric field because Stark shifts of the upper and lower levels cancel out. By contrast, the $R(1/2)$ transition splits into two as shown in Fig. 4(b). Frequencies of both Stark transitions increase with increasing electric field. We calculated the optical Stark potential of CaF in a varying electric field and found that it only changes by of 0.045% when the electric field varies from 0 kV/cm to 100 kV/cm.

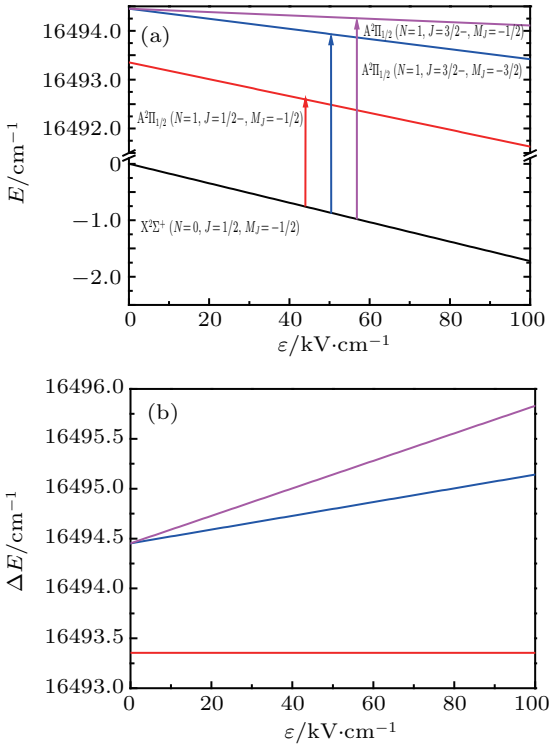


Fig. 4. (a) Stark shifts of the levels of interest of CaF varying with applied electric fields, together with the allowed Stark transitions (arrows). (b) Frequencies of the transitions corresponding to the denoting arrows in panel (a) varying with applied fields.

On the other hand, the optical Stark potential does vary when the molecule travels in the decelerator due to the Doppler effect. When the molecule travels at a velocity of υ against the laser beam, the laser frequency which the molecules *see* becomes $(\nu + \upsilon/\lambda)$, where λ is the laser wavelength. In this

case, equation (4) must be modified as,

$$V = -\frac{q_{00}d^2E_{\rm L}^2}{4h}\sum_i \frac{f_i \cdot S_J}{\nu_{ij} - (\nu + \upsilon/\lambda)}. \tag{5}$$

As the molecule is gradually slowed in the decelerator, the real detuning frequency increases, resulting in less bunching of the assisting laser beam to the molecule. Therefore, the laser frequency needs to be tuned synchronously for the most efficient laser deceleration.

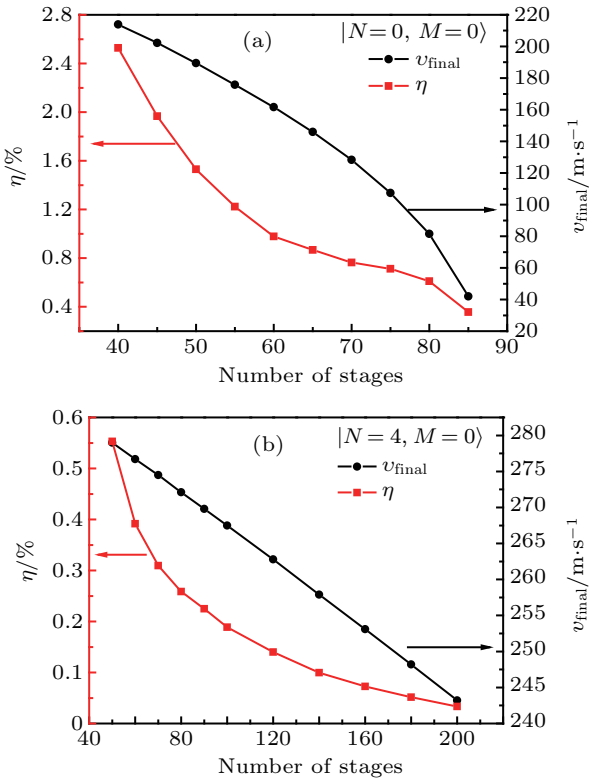


Fig. 5. (a) Monte-Carlo simulation of the relative molecular number (η) and the obtained velocity of CaF in its HFS $|N=0, M=0\rangle$ state as functions of the deceleration stages using the near-red-detuning laser-assisted Stark deceleration method. The assisting laser frequency is fixed at 5.0 GHz red-detuned to the $Q(1/2)$ transition, and the laser power density is 10^5 W/cm^2. (b) Simulation of CaF in its LSF $|4,0\rangle$ using the traditional Stark deceleration method for comparison. The electrostatic field is switched at the phase of $-60°$ and $60°$, respectively.

A Monte-Carlo simulation has been performed with the assisting laser frequency red-detuned by 5.0 GHz from the $Q(1/2)$ transition (ν = 16493.3539 cm^{-1}) of the (0, 0) band in the A–X system of CaF and the intensity set at $I = 1 \times 10^5$ W/cm^2 ($\sim$ 5.6 W), which produces a transverse bunch potential over 70 mK (while the transverse temperature of the molecules beam is about 10 mK[38]). The parameters of the assisting laser are set as constant unless otherwise stated. The initial velocity of the molecules passing through the skimmer is set as centered at 290 m/s with an full width at half maximum (FWHM) of 80 m/s. The velocity of the decelerated molecular package and the relative molecular number η, defined as the ratio of the decelerated molecules to the incident molecules, as functions of the number of deceleration stages are plotted in Fig. 5(a). The electrostatic field is switched at the phase angle[37] of $-60°$. Figure 5(b) plots the simulation of traditional Stark deceleration (the electrostatic field switched at the phase angle of 60°) of CaF in its LSF $|4,0\rangle$ state for comparison. Evidently, both the bunching ratio and the deceleration efficiency of the present scheme are better.

The time-of-flight (TOF) signals of the decelerated molecular packages can visually support the above conclusion, and thus, are plotted in Fig. 6. The TOF signals of the present scheme are plotted in red while those of the traditional are in black. The features of the signals in Fig. 6 are listed in Table 1. Through 85 deceleration stages, for example, the present obtained molecular package velocity and relative number are 42.0 m/s and 0.36% (peak H), respectively, while they are 271.1 m/s and 0.23% (peak h), respectively, using the traditional scheme.

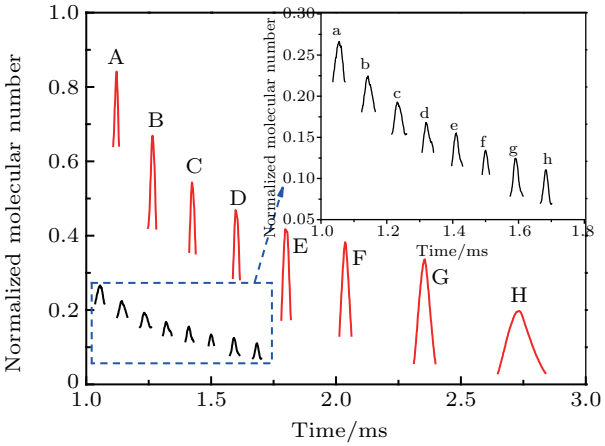


Fig. 6. Simulated normalized TOF signals of the present decelerated molecular package of the $|0,0\rangle$ CaF (in red) and those of $|4,0\rangle$ of the traditional one (in black) after different deceleration stages. Peaks A to H (or a to h) represent stages from 50 to 85 with the step of 5. The inset (magnified peaks of the weak ones in the left-bottom) shows clearly the normalized molecular numbers.

Table 1. Velocities and relative molecular numbers of the molecular packages at different deceleration stages.

Stages	$\|0,0\rangle$ (present)			$\|4,0\rangle$ (traditional)		
	Peak	υ/(m/s)	η/%	Peak	υ/(m/s)	η/%
50	A	189.5	1.53	a	279.0	0.55
55	B	175.8	1.22	b	277.9	0.45
60	C	161.7	0.98	c	276.7	0.39
65	D	146.0	0.87	d	275.6	0.33
70	E	128.3	0.76	e	274.5	0.31
75	F	107.4	0.71	f	273.3	0.28
80	G	81.5	0.61	g	272.1	0.25
85	H	42.0	0.36	h	271.1	0.23

The complete molecular TOF signals after 80 deceleration stages of the present (in red) and the traditional (in black) are plotted in Fig. 7, where the down arrows denote the molecular packages of interest. In addition, the phase-space acceptance through 80 slowing stages of the two compared schemes,

as shown in the insets in Fig. 7, further suggests the superiority of our scheme over the traditional one. Evidently, our phase-space acceptance is stable while the traditional phase-space distribution has not yet become stable through 80 slowing stages. Simulation illustrates that the phase-space distribution of the $|4,0\rangle$ level CaF molecules via traditional Stark deceleration cannot be stable until through 150-stage slowing.

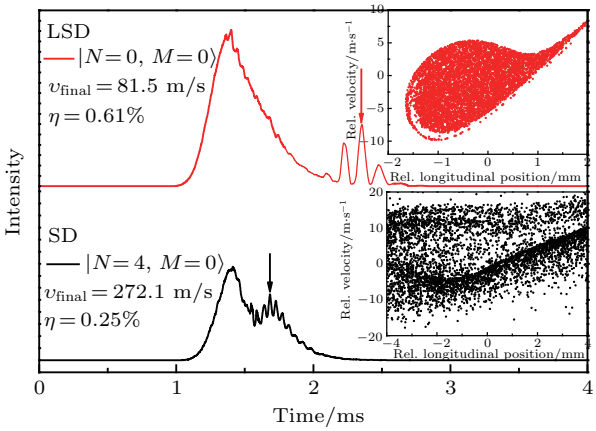


Fig. 7. TOF signals of the present laser-assisted Stark deceleration (LSD) scheme (in red) of the $|0,0\rangle$ state and of the traditional Stark deceleration (SD) scheme (in black) of the $|4,0\rangle$ state of CaF molecules after 80 deceleration stages, where the down arrows denote the slowed molecular packages, and the achieved velocity ($v_{\rm final}$), and the relative molecules (η) of the two schemes are also denoted. The insets plot the phase-space acceptance of the two compared schemes after 80 slowing stages.

The relative molecular number depends closely on the optical Stark potential generated by the assisting laser beam. Figure 8 plots the relative molecular number through 80 slowing stages varying with the optical Stark potential employing our scheme. Our simulation shows that there is an optional potential to obtain the largest relative molecular number. The large decreasing of the relative molecular number at higher potential may arise from the over focusing of the molecular beam in transverse. The optional optical potential is around -112 mK in our simulation condition (the molecular transverse temperature is typically to be 10 mK). If we set the assisting laser frequency to be 5.0 GHz red-detuned to the molecular transition, the laser power density is 1.75×10^5 W/cm^2, corresponding to the power of 9.8 W. If we set the laser frequency red-detuning to be 1.0 GHz, then the laser power will reduce to be 1.2 W.

The HFS $|0,0\rangle$ state of CaF can also be slowed using AG Stark deceleration method[35] although its electrodes are difficult to align experimentally and its stages can hardly more than 21 (increasing of stages more than 13 will give rise to continuous losses of molecules[36]). Nevertheless, we still compare our scheme with the AG one. Figure 9 plots the relative molecular number versus deceleration stages of these two methods, where the black is the AG from Ref. [36] and the red is the present simulation results. The large fluctuation of Ref. [36] may arise from the miss-alignment of the electrostatic electrodes. We can basically conclude that, when decelerated over 20 stages, the present method would obtain more molecules than the AG method. Furthermore, after 21 stages, the present molecules will lose 23.3% of their kinetic energy, while they will only lose 15.1% in the AG one despite its higher ($\pm$20 kV/cm, twice of the present) voltages applied.

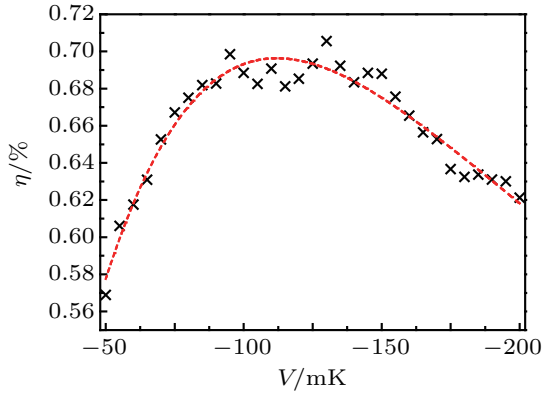


Fig. 8. Monte-Carlo simulation of the relative molecular number η of $|N=0,M=0\rangle$ CaF varying with the optical Stark potential V of the assisting laser after 80 slowing stages via laser-assisted Stark deceleration.

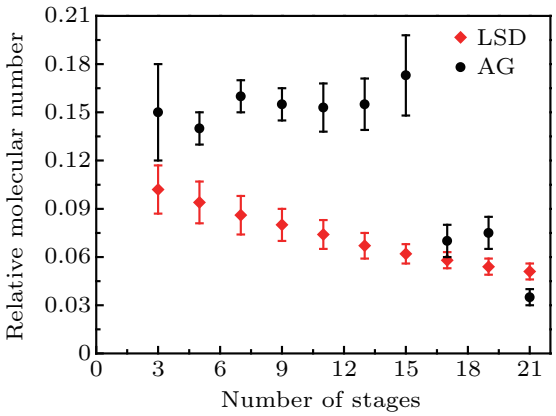


Fig. 9. Relative molecular number varying with the declaration stages of our Monte-Carlo simulation of the present laser-assisted Stark deceleration (LSD) scheme (red) and the alternating gradient (AG) Stark deceleration experimental[36] (black).

Our simulation suggests that the rovibronic ground state CaF would be decelerated to be 27.3 m/s with the relative molecular number of 0.26% when decelerated by 86 stages using the present scheme, and the equivalent temperature is about 2.3 mK. In other words, about 2.6×10^4 cold molecules with the density of 8.3×10^8 cm^{-3} at 2.3 mK would be achieved under the typical experimental condition (the number of the CaF passing through the skimmer to be at the order of 10^7[46]). Note that Eqs. (2)–(4) is treated at the second-order perturbation limited. If the third-order perturbation correction is taken into account, the guiding potential will shift less than 10%, resulting in the relative slowed molecular number varying at the order of 10^{-2}. Another possible molecular loss is due to the photon scattering of the assisting laser beam during the slowing process. Each molecule could scatter about 10^4 photons during the slowing time of about 3 ms, but only

a small fraction of the molecules will be scattered to other rotational levels (thus, lost in the process) via Raman (Stokes) scattering. This will not affect the simulated results much.

The dimension of the slowed molecular package is about 4.0 mm longitudinally and 0.1 mm in diameter transversely (as shown in the upper inset in Fig. 7), and if trapped in a 3D optical trap, it could be greatly suppressed longitudinally, which might increase the density about a factor of 40. This is comparable with the latest experimental results, which are a molecular number and density to be $1.0(3)\times10^5$ cm^{-3} and $7(3)\times10^6$ cm^{-3}, respectively, at a temperature of 340(20) μK achieved experimentally by direct laser cooling method in an MOT in the group of Doyle.[47] Furthermore, the incident molecular flux can be enhanced by a factor of 30 if we cool the skimmer to 8 K to suppress its clogging, as demonstrated most recently in the group of Ye.[48] Additionally, by properly adjusting the assisting laser parameters, more cold molecules would be achieved.

As mentioned earlier, the assisting laser power is about 5.6 W under our simulation conditions, which is feasible in experiment. To further decrease the laser power desired, we can reduce the frequency detuning. If we tune the laser frequency to keep the real detuning invariable to be 1.0 GHz (much larger than the spectral neutral broadening about 8.3 MHz,[49] where the Doppler and collision broadening can be neglected in this case) in the course of the slowing process, the power of the assisting laser of only 1.2 W would result in a relative molecular number of 0.25% after 86 stages.

The slowed HFS molecules at the end of the decelerator can be trapped in a 3D all-optical trap, which can be formed by this assisting laser beam and another crossed laser beam. The loading of the molecules into this trap and further evaporative cooling are currently under investigation in our group.

4. Conclusions

A near-resonant, red-detuning laser-assisted Stark deceleration scheme is proposed to slow rovibronic ground (HFS) state CaF molecules. Our simulations suggest that a number and a density at the order of 10^4 cm^{-3} and 10^8 cm^{-3}, respectively, cold CaF molecules at an equivalent temperature of 2.3 mK would be achieved under typical experimental conditions. These results are comparable with those of the latest experiment achieved by direct laser cooling of CaF in an MOT.[47] The higher density of cold molecules would have wide applications and would be essential for further cooling. In contrast to the previous proposals of far-red-detuning laser-assisted method,[37,38] the present assisting laser power would be as low as about 1.2 W when keeping the real red-detuning to 1.0 GHz, which is feasible experimentally.

Acknowledgment

We are grateful to Prof. Jun Ye at JILA, University of Colorado and Prof. Michael R Tarbutt at Imperial College London for their valuable discussions.

References

[1] Micheli A, Brennen G K and Zoller P 2006 *Nat. Phys.* **2** 341
[2] Goral K, Santos L and Lewenstein M 2002 *Phys. Rev. Lett.* **88** 170406
[3] Yelin S F, Kirby K and Côté R 2006 *Phys. Rev. A* **74** 050301
[4] DeMille D 2002 *Phys. Rev. Lett.* **88** 067901
[5] Lee C and Ostrovskaya E A 2005 *Phys. Rev. A* **72** 062321
[6] Krems R V 2005 *Int. Rev. Phys. Chem.* **24** 99
[7] Krems R V 2004 *Phys. Rev. Lett.* **93** 013201
[8] Schiller S 2007 *Phys. Rev. Lett.* **98** 180801
[9] Demille D, Sainis S, Sage J, Bergeman T, Kotochigova S and Tiesinga E 2008 *Phys. Rev. Lett.* **100** 043202
[10] Zelevinsky T, Kotochigova S and Ye J 2008 *Phys. Rev. Lett.* **100** 043201
[11] Hudson E R, Lewandowski H J, Sawyer B C and Ye J 2006 *Phys. Rev. Lett.* **96** 143004
[12] Bohn J L, Rey A M and Ye J 2017 *Science* **357** 1002
[13] Dhont G S F, Lenthe J H V, Groenenboom G C and van der Avoird A 2005 *J. Chem. Phys.* **123** 184302
[14] Janssen L M C, Groenenboom G C, van der Avoird A, Żuchowski P S and Podeszwa R 2009 *J. Chem. Phys.* **131** 224314
[15] Manai I, Horchani R, Lignier H, Pillet P and Comparat D 2012 *Phys. Rev. Lett.* **109** 183001
[16] Zhelyazkova V, Cournol A, Wall T E, Matsushima A, Hudson J J, Hinds E A, Tarbutt M R and Sauer B E 2014 *Phys. Rev. A* **89** 053416
[17] Wan M G, Yuan D, Jin C G, Wang F H, Yang Y J, Yu Y and Shao J X 2016 *J. Chem. Phys.* **145** 024309
[18] Bethlem H L, Berden G and Meijer G 1999 *Phys. Rev. Lett.* **83** 1558
[19] Bochinski J R, Hudson E R, Lewandowski H J, Meijer G and Ye J 2003 *Phys. Rev. Lett.* **91** 243001
[20] Hudson E R, Ticknor C, Sawyer B C, Taatjes C A, Lewandowski H J, Bochinski J R, Bohn J L and Ye J 2006 *Phys. Rev. A* **73** 063404
[21] van de Meerakker S Y T, Labazan I, Hoekstra S, Küpper J and Meijer G 2006 *J. Phys. B: At. Mol. Opt. Phys.* **39** S1077
[22] Narevicius E, Libson A, Parthey C G, Chavez I, Narevicius J, Even U and Raizen M G 2008 *Phys. Rev. Lett.* **100** 093003
[23] Wiederkehr A W, Hogan S D and Merkt F 2010 *Phys. Rev. A* **82** 043428
[24] Vanhaecke N, Meier U, Andrist M, Meier B H and Merkt F 2007 *Phys. Rev. A* **75** 031402
[25] Doyle J M, Friedrich B, Kim J and Patterson D 1995 *Phys. Rev. A* **52** R2515
[26] Bethlem H L, Berden G, Crompvoets F M H, Jongma R T, van Roij A J and Meijer G 2000 *Nature* **406** 491
[27] Zeppendeld M, Motsch M, Pinkse P W H and Rempe G 2009 *Phys. Rev. A* **80** 041401
[28] Prehn A, Ibrügger M, Glöckner R, Rempe G and Zeppendeld M 2016 *Phys. Rev. Lett.* **116** 063005
[29] Steinecker M H, McCarron D J, Zhu Y Q and DeMille D 2016 *Chem. Phys. Chem.* **17** 22
[30] Norrgard E B, McCarron D J, Steinecker M H, Tarbutt M R and DeMille D 2016 *Phys. Rev. Lett.* **116** 063004
[31] McCarron D J, Norrgard E B, Steinecker M H and DeMille D 2015 *New J. Phys.* **17** 035014
[32] Williams H J, Truppe S, Hambach M, Caldwell L, Fitch N J, Hinds E A, Sauer B E and Tarbutt M R 2017 *New J. Phys.* **19** 113035
[33] Tokunaga S K, Dyne J K, Hinds E A and Tarbutt M R 2009 *New. J. Phys.* **11** 055038
[34] Bethlem H L, Crompvoets F M H, Jongma R T, van de Meerakker S Y T and Meijer G 2002 *Phys. Rev. A* **65** 053416
[35] Bethlem H L, van Roij A J, Jongma R T and Meijer G 2002 *Phys. Rev. Lett.* **88** 133003
[36] Wall T E, Kanem J F, Dyne J M, Hudson J J, Sauer B E, Hinds E A and Tarbutt M R 2011 *Phys. Chem. Chem. Phys.* **13** 18991
[37] Huang Y X, Xu S W and Yang X H 2016 *J. Phys. B: At. Mol. Opt. Phys.* **49** 135101

[38] Chen K, Huang Y X and Yang X H 2017 *Chin. J. Chem. Phys.* **30** 418
[39] Hanna D C, Yuratich M A and Cotter D 1979 *Nonlinear optics of free atoms, molecules* (Berlin: Springer-Verlag)
[40] Fieid R W, Harris D O and Tanaka T 1975 *J. Mol. Spectrosc.* **57** 107
[41] Nakagawa J, Domaille P J, Steimle T C and Harris D O 1978 *J. Mol. Spectrosc.* **70** 374
[42] Childs W J, Goodman L S, Nielsen U and Pfeufer V 1984 *J. Chem. Phys.* **80** 062283
[43] Wall T E, Kanem J F, Hudson J J, Sauer B E, Cho D, Boshier M G, Hinds E A and Tarbutt M R 2008 *Phys. Rev. A* **78** 062509
[44] Raouafi S, Jeung G H and Jungen C 2001 *J. Chem. Phys.* **115** 7450
[45] Hemmerling B, Chae E, Ravi A, Anderegg L, Drayna G K, Hutzler N R, Collopy A L, Ye J, Ketterle W and Doyle J M 2016 *J. Phys. B: At. Mol. Opt. Phys.* **49** 174001
[46] Lu H, Rasmussen J, Wright M J, Patterson D and Doyle J M 2011 *Phys. Chem. Chem. Phys.* **13** 18986
[47] Anderegg L, Augenbraun B L, Chae E, Hemmerling B, Hutzler N R, Ravi A, Collopy A L, Ye J, Ketterle W and Doyle J M 2017 *Phys. Rev. Lett.* **119** 103201
[48] Wu H, Reens D, Langen T, Shagam Y, Fontecha D and Ye J 2018 *Phys. Chem. Chem. Phys.* **20** 11615
[49] Tarbutt M R and Steimle T C 2015 *Phys. Rev. A* **92** 053401